Broad-Band All-Optical Wavelength Conversion of Differential Phase-Shift Keyed Signal Using an SOA-Based Nonlinear Polarization Switch

Ya-Ya Mao(毛雅亚), Xin-Zhi Sheng(盛新志), Chong-Qing Wu(吴重庆)**, Kuang-Lu Yu(余贶琭)

Institute of Optical Information, and Key Lab of Luminescence and Optical Information Technology (Ministry of Education), Beijing Jiaotong University, Beijing 100044

(Received 13 November 2015)

Broad-band all-optical wavelength conversion of differential phase-shift keyed (DPSK) signal is experimentally demonstrated. This scheme is composed of a one-bit delay interferometer demodulation stage followed by a semiconductor optical amplifier (SOA) based nonlinear polarization switch. A wavelength converter for the 10 Gb/s DPSK signal is presented, which has a wide wavelength range of more than 30 nm. The converted signals experience small power penalties less than 1.4 dB compared with the original signal, at a bit error rate of 10^{-9}. Additionally, the optical spectra, the measured waveforms and the open eye diagrams of the converted signals show a high quality wavelength conversion performance.

PACS: 42.79.Sz, 42.25.Kb, 42.65.Yj, 42.65.Re DOI: 10.1088/0256-307X/33/3/034204

All-optical wavelength conversion is considered to be a key function performed at the nodes of wavelength division multiplexing (WDM) networks.[1] Among the methods available, the converters that use semiconductor optical amplifiers (SOAs) are considered to be the most promising scheme due to their advantages of high non-linear effect and easy integration. However, great efforts have been made with wavelength converters for on-off keying (OOK) signals,[2–6] and these schemes predominantly concentrate on amplitude replication alone. Due to their improved receiver sensitivity of balanced detection, differential phase-shift keyed (DPSK) formats attract much attention due to their lower optical signal-to-noise ratio (OSNR) requirements and higher tolerance to nonlinear effects compared to the OOK formats.[7,8] Therefore, all-optical wavelength converters for DPSK signals should be further explored. Some solutions that exploit four-wave mixing (FWM) in SOA, which can preserve both phase and amplitude information, have been designed.[9–13] Unfortunately, these existing solutions only offer a restricted wavelength conversion range and require a high pump optical power. Recently, DPSK signal converters comprising of a one-bit delay interferometer (DI) demodulator followed by an SOA based Mach–Zehnder interferometer (SOA-MZI) have been shown to provide wavelength conversion with high power efficiency and a large conversion wavelength range.[14–16] However, in an SOA-MZI, the control signals that are injected need to be exactly time correlated. In this Letter, a new wavelength converter is proposed and experimentally demonstrated, which comprises a DI demodulator followed by an SOA-based nonlinear polarization switch. The proposed scheme has the advantages of a large wavelength conversion range and a simple structure.

The experimental setup of the DPSK wavelength conversion is illustrated in Fig. 1. A 10 Gb/s DPSK signal with a wavelength of 1545.08 nm is generated by modulating an external Mach–Zehnder modulator (MZM) driven by an electrical non-return-to-zero (NRZ) data stream from a pulse pattern generator (PPG, model MP1800A, Anritsu). The DPSK signal is optimized by adjusting the first polarization controller (PC1), and then converted into an OOK signal with a one-bit DI. The OOK signal is amplified by an erbium-doped fiber amplifier (EDFA) and is coupled into the SOA via the circulator as a control signal, whose power is strong enough to introduce nonlinear effects of the SOA. A probe light with a target wavelength of 1550.12 nm is injected into the SOA as a probe signal, which is too weak to cause nonlinearity of the SOA. PC2 is used to adjust polarization of the probe light to be approximately 45° to the orientation of the SOA layers.[17]

The nonlinear polarization switch plays an essential role in the wavelength conversion. As shown in the dashed box of Fig. 1, it consists of several parts: an SOA, an optical circulator, an optical bandpass filter (BPF), a polarization controller (PC3) and a polarization beam splitter (PBS). The SOA (Model ISPAD1501, InPhenix) is with 100 ps recovery time, and the BPF is with 0.8 nm bandwidth. The probe light interacts with the OOK signal through cross-gain modulation (XGM) and cross-phase modulation (XPM) effects in the SOA. By adjusting the control signal power and the bias current of SOA, the nonlinear phase shift difference of the probe light can reach π when the control signal converts between '0' and '1'. Then the probe light picks up the phase infor-

**Corresponding author. Email: cqwu@bjtu.edu.cn

© 2016 Chinese Physical Society and IOP Publishing Ltd

mation. However, when the phase of the probe light changes, the amplitude of the probe light also changes due to XGM. Thus the 1 and 0 signals have different amplitudes at the output of the SOA. Therefore, an amplitude equalizer is required for the conversion. The working principle of the equalizer used in the conversion is based on the nonlinear polarization rotation (NPR) in the SOA. When the control signal is coupled into the SOA, the probe light rotates due to a phase shift difference between the transverse electric (TE) and transverse magnetic (TM) modes in the SOA, and the state of polarization (SOP) of the probe light rotates by a smaller angle when the control signal is 0 than that when the control signal is 1. The PC3 combined with PBS is used as a polarizer, which is adjusted to obtain a constant probe amplitude output. The other one-bit DI is used to demodulate the converted signal. An optical spectrum analyzer (OSA, Model AQ-6317, ANDO) with a 0.016 nm resolution and a 28 GHz sampling oscilloscope (OSC, Model WaveExpert 100H, LeCroy) are used to observe the signal spectrum and the waveform, respectively.

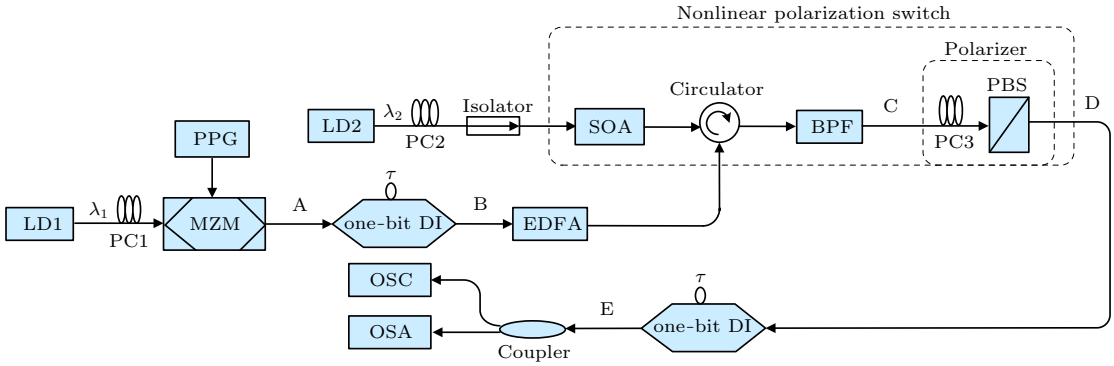

Fig. 1. Structure of the wavelength converter based on an SOA-based nonlinear polarization switch.

To optimize the performance of the converter, the gain of the SOA for different input signal powers is measured, as shown in Fig. 2(a), and the phase shift and rotation azimuth of the signal are calculated, as shown in Figs. 2(b) and 2(c), respectively. The bias currents of SOA are set at 120 mA, 150 mA and 180 mA, respectively. The phase shift and rotation azimuth of the signal were calculated via[17,18]

$$\varphi = -\frac{1}{2}\bar{\alpha}\ln[G], \tag{1}$$

$$\theta = 0.115 \cdot \Delta\alpha \cdot [10\ln G - 10\ln G_0], \tag{2}$$

where φ is the phase shift, $\bar{\alpha}$ is the average linewidth enhancement factor of the TE and TM modes, with a value of 5.0, G is the gain of the SOA, θ is the rotation azimuth, $\Delta\alpha$ with a value of 0.85 is the difference linewidth enhancement factor between the TE and TM modes, and G_0 is the small signal gain of the SOA. As shown in Fig. 2, when the bias current of SOA is 180 mA and the input signal power is −7 dBm, the gain, the phase shift and the rotation azimuth of the signal are approximately 9.5, -1.8π and 0.7 rad, respectively. With the same bias current but a different input signal power of 3 dBm, the gain, the phase shift and the rotation azimuth of the signal become approximately 2.7, -0.8π and 1.9 rad, respectively. In this experiment, the input signal power of the SOA is composed of the probe light power and the control signal power. Based on the above analysis, we select the bias current of the SOA as 180 mA, the optical powers of the probe light and the control signal as −7 dBm and 2.6 dBm, respectively, which can ensure that the phase shift difference of the probe light reaches π when the control signal converts between 0 and 1. Under these conditions, the included angle of the probe signal between signals 0 and 1 is 1.2 rad. By adjusting the polarizer to the position as shown in the inset of Fig. 2, a constant optical power output from the polarizer can be obtained.

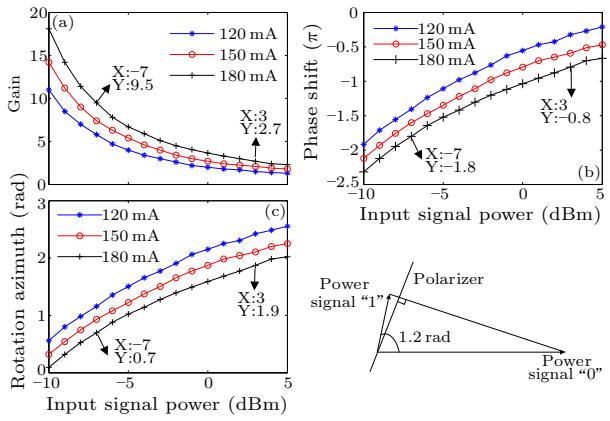

Fig. 2. Gain, phase shift and rotation azimuth as a function of the input signal power.

In the experiment, the data signal is programmed with pseudo-random binary sequences (PRBS) of length $2^{31}-1$. The left column of Fig. 3 shows the waveforms of the signals at 10 Gb/s at positions A–E in Fig. 1, and the corresponding eye diagrams are shown in the right column. The original and the demodulated DPSK signals are measured at positions

A and B, and the results are shown in Figs. 3(a) and 3(b), respectively. In the experiment, the NRZ-DPSK signal is generated by using MZM, which causes the power dips to appear in the NRZ-DPSK signal, as shown in Fig. 3(a). Figure 3(c) gives the waveform and the eye diagram of the probe light at position C. Variations in the amplitude of the probe light can be seen due to XGM by the control signal. The waveform and eye diagram of the converted signal at position D are shown in Fig. 3(d), and the optical power of signal 1 is equalized with the signal 0. Since the control signal is not a perfect rectangular signal, the converted signal has slight amplitude fluctuations at the rising and falling edges. Figure 3(e) gives the waveform and eye diagram of the demodulated converted signal. The clear and open eye diagrams of the demodulated converted signal demonstrate the high quality wavelength conversion performance. Since the control OOK signal results from an exclusive or (XOR) function between subsequent bits of the original DPSK signal, this scheme alters the encoding of the obtained signal. Therefore, the obtained signal is actually a PSK signal. However, this change in data encoding can be addressed by the post-decoding data processing. In this experiment, a pre-coder and a post-decoder were not required since a PRBS was used. This converter has the potential to be used at higher bit rate. However, in the present experiment we were limited by the speed of our signal source and the carrier recovery time of the SOA, and the converter was operated at 10 Gb/s.

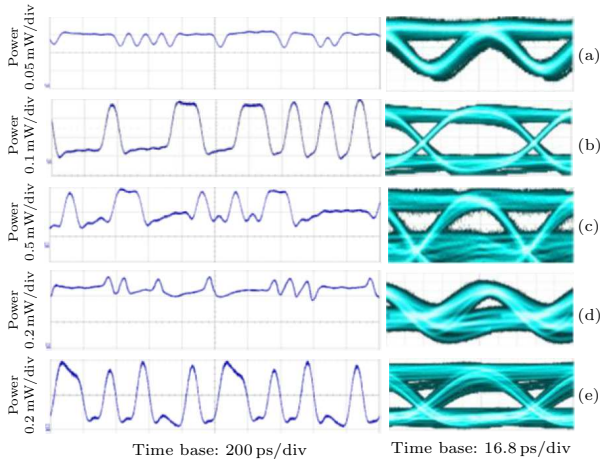

Fig. 3. Waveforms and eye diagrams of (a) the original DPSK signal, (b) the demodulated DPSK signal, (c) the signal output from SOA, (d) the converted signal, and (e) the demodulated converted signal.

The measured spectra are shown in Fig. 4. Figure 4(a) shows the spectrum of the original probe light with a wavelength of 1550.12 nm, and the spectrum of the converted signal is shown in Fig. 4(b). The bandwidth of the probe light is broadened due to the modulation by the control signal. The inset shows the detailed spectrum of the converted signal.

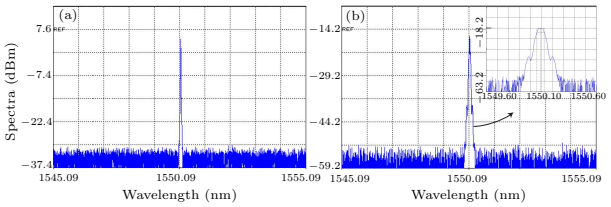

Fig. 4. Measured spectra of (a) the original probe light and (b) the converted signal.

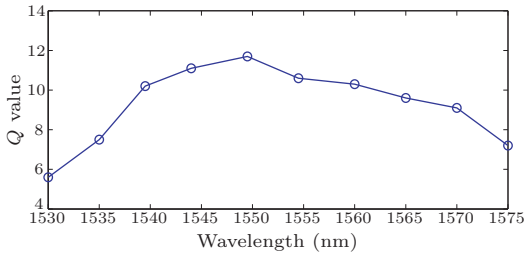

Fig. 5. The Q value for the converted signal against the probe wavelength.

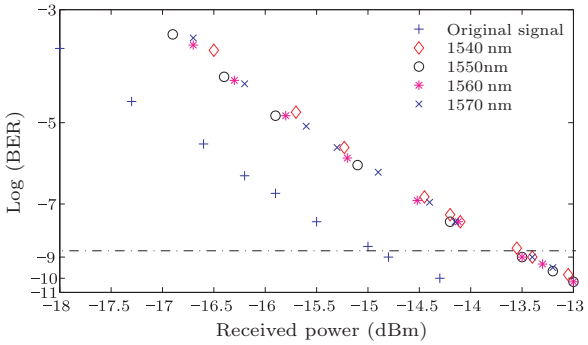

Fig. 6. BER characteristics for the converted signal and the original DPSK signal.

The dependence of the conversion performance on the wavelengths of the probe light was also investigated. The Q value for the converted signal at different probe wavelengths is shown in Fig. 5. When the original signal wavelength is fixed at 1545.08 nm, the Q values greater than 9 can be achieved within a wide probe wavelength range from 1540 nm to 1570 nm. Due to constraints of the gain bandwidth of the SOA used in this experiment, the conversion performance degrades when the probe wavelength is less than 1535 nm or more than 1575 nm, as shown in Fig. 5. The wide conversion bandwidth is ideal for extension of our application to wavelength multicasting of the DPSK signal.

Being processed by a one-bit DI, the signal has been demodulated for evaluation. The bit error rate (BER) characteristics of the converted signals are measured in comparison with the original DPSK signal. The wavelength of the original DPSK signal is 1545.08 nm, and the wavelengths of the probe light are 1540 nm, 1550 nm, 1560 nm and 1570 nm, respectively. As shown in Fig. 6, the converted signals with

different wavelengths at the BER of 10^{-9} have power penalties less than 1.4 dB compared with the original DPSK signal. This small penalty indicates a high quality system performance.

In summary, we have experimentally demonstrated a 10 Gb/s DPSK signal wavelength conversion scheme based on an SOA-based nonlinear polarization switch. The experimental results show that the scheme can be used with a wide wavelength conversion range over 30 nm. For all probe wavelengths tested, the converted signals experience small power penalties less than 1.4 dB at BER of 10^{-9} compared with the original signal. The optical spectra, the measured waveforms and the open eye diagrams of the converted signal show a high quality wavelength conversion performance as well.

References

[1] Willner A E, Khaleghi S, Chitgarha M R and Yilmaz O F 2014 *J. Lightwave Technol.* **32** 660

[2] Wang W, Poulsen H N, Rau L, Chou H F, Bowers J E and Blumenthal D J 2005 *J. Lightwave Technol.* **23** 1105

[3] Girault G and Clarke A M 2008 *Opt. Commun.* **281** 5731

[4] Fu S and Dong J 2006 *Opt. Express* **14** 7587

[5] Guo L Q and Connelly M J 2008 *Opt. Commun.* **281** 4470

[6] Liu J and Cheng T H 2008 *Opt. Commun.* **281** 5415

[7] Gnauck A H and Winzer P J 2005 *J. Lightwave Technol.* **23** 115

[8] Winzer P J and Essiambre R 2006 *J. Lightwave Technol.* **24** 4711

[9] Hu H and Palushani E 2010 *Opt. Express* **18** 9961

[10] Schmeckebier H and Meuer C 2012 *IEEE Photon. Technol. Lett.* **24** 1163

[11] Porzi C and Bogoni A 2013 *IEEE Photon. Technol. Lett.* **25** 175

[12] Matsuura M and Kishi N 2011 *IEEE Photon. Technol. Lett.* **23** 615

[13] Li Z and Dong Y 2004 *IEEE Photon. Technol. Lett.* **16** 1685

[14] Wang J, Maitra1 A, Freude W and Leuthold J 2009 *Opt. Express* **17** 22639

[15] Wei H, Li M, Zhang X, Sun J and Huang D 2009 *J. Lightwave Technol.* **27** 5580

[16] Vorreau P and Marculescu A 2006 *IEEE Photon. Technol. Lett.* **18** 1970

[17] Zhao S, Wu C, Cheng M, Li Z and Feng Z 2009 *IEEE J. Quantum Electron.* **45** 1006

[18] Agrawal G P and Olsson N 1989 *IEEE J. Quantum Electron.* **25** 2297